

Magic state distillation from entangled statesNing Bao,^{1,*} ChunJun Cao,^{2,†} and Vincent Paul Su^{3,‡}¹*Computational Science Initiative, Brookhaven National Laboratory, Upton, New York 11973, USA*²*Joint Center for Quantum Information and Computer Science, University of Maryland, College Park, Maryland 20742, USA*³*Center for Theoretical Physics and Department of Physics, University of California, Berkeley, California 94720, USA*

(Received 26 July 2021; accepted 22 December 2021; published 3 February 2022)

Magic can be distributed nonlocally in many-body entangled states, such as the low energy states of condensed matter systems. Using the Bravyi-Kitaev magic state distillation protocol, we find that nonlocal magic is distillable and can improve the distillation outcome. We analyze a few explicit examples and show that spin squeezing can be used to convert nondistillable states into distillable ones. Our analysis also suggests that the conventional product input states assumed by magic distillation protocols are extremely atypical among general states with distillable magic. It further justifies the need for studying a diverse range of entangled inputs that yield magic states with high probability.

DOI: [10.1103/PhysRevA.105.022602](https://doi.org/10.1103/PhysRevA.105.022602)**I. INTRODUCTION**

Fault tolerance is an absolute necessity for leveraging the full power of quantum computing. It is known that one cannot implement a universal set of gates transversally using a single quantum error correction code [1–5]. For many popular choices of codes, Clifford gates are often transversal while the non-Clifford gates are not. Therefore, the challenge is to perform the remaining non-Clifford element, such as a T gate, fault tolerantly. The difficulty of implementing these T gates forms a major bottleneck for the development of universal quantum computation. Various solutions for implementing non-Clifford gates have been proposed [6–14].

One such proposal is to prepare so-called “magic states” and perform T gates through measurement-based quantum computation schemes [6,15–17] using only fault-tolerant Clifford operations. To this end, magic state distillation (MSD) protocols have been developed in order to convert product states with large overlap with the magic states into the magic states of a particular form; for the seminal work in this area, please see [6,7]. However, these magic states can be costly to prepare with arbitrarily high accuracy. Such is the prevalent assumption behind the program of Clifford+T circuit decompositions and related compilation schemes [18–22]. Because of the inefficiencies in distilling these magic states, the ability to develop a “magic state factory” that is capable of effectively generating such states in large quantities would be a great advance to the scalability of quantum computation. For an alternate approach to fault tolerant computation using code switching, see [23–28].

The conventional setup for magic state distillation takes a number of noisy ancillae, which are often represented as

product of identical single qubit mixed states, and projects them onto the code subspace of a carefully chosen quantum error correction code. One then decodes using a fault-tolerant Clifford circuit and obtains a number of magic states that have higher fidelity provided the inputs are above a distillation threshold. A great number of procedures and variants have been devised to various degrees of efficacy [6,7,29–33].

While the product of identical mixed states is a natural input state, its form is rather restrictive considering the vast pool of many-body quantum states that occur naturally in physical systems that can function as magic reservoirs [34–38]. In particular, recent progress in quantum many-body magic indicates that magic, like entanglement, can take on various forms in such states. Indeed, while some of the magic is found locally, not unlike the conventional input states in magic distillation protocols, a large portion remains in the correlations and is distributed nonlocally in entangled states. Therefore, it is natural to ask whether such “nonlocal” magic from these systems can be (a) distilled and (b) used to improve the outcome of distillations. More generally, it is beneficial, not only theoretically but also practically, to understand how MSD performs on a much wider class of inputs, where magic is not concentrated strictly locally on each ancilla.

In this work, we take a step in characterizing how more generic input states, such as entangled states, can alter the outcomes of distillation. In particular, we answer both of the above questions in the affirmative: it is possible to distill magic that is distributed nonlocally, as opposed to locally in the traditional input states. Nonlocal magic (NLM) can also improve the success probabilities of the distillation protocol. A wider range of input states can thus help reduce the overall cost for generating a much needed quantum resource. From a practical perspective, we show that well-known procedures used in spin squeezing that generate entanglement and non-local magic can render undistillable magic states distillable. More concretely, we conduct our explicit analysis using the Bravyi-Kitaev (BK) magic distillation protocol [6] and study

*ningbao75@gmail.com

†ccj991@gmail.com

‡vipasu@berkeley.edu

how it performs over different forms of entangled five-qubit states.

We will review some basic aspects of magic states and their distillation in Sec. II. Then in Sec. III we construct different entangled states with varying magic distributions and perform the Bravyi-Kitaev protocol for T state distillation using these as input states. We show that, although the conventional form of input states explicitly have only single qubit magic, states with purely nonlocal magic such that individual qubit reduced density matrices look nonmagical can remain fully distillable. We then consider both conceptually simple and practically relevant examples where nonlocal magic and entanglement improve distillation outcome. This is made particularly apparent with the example of spin squeezing, where nondistillable states are rendered distillable with a slight addition of nonlocal magic and entanglement. Then in Sec. IV we further analyze the properties that make certain states more distillable from the point of view of the quantum error correction code in question. By analyzing random distillable states, we conclude that the conventional MSD inputs are extremely atypical whereas typical distillable states have high entanglement and zero local magic. We then provide some intuitions for the patterns behind the distribution of the distillable states. Finally, in Sec. V, we summarize our findings, speculations, and future directions.

II. BACKGROUND

A. Magic

Stabilizer states are generated by Clifford operations acting on the all zeros state. They have a wide range of applications in quantum information, condensed matter physics, and quantum gravity [39–41]. However, it is well known that they are not dense in the Hilbert space, and thus the Clifford operations, which can be implemented transversally for certain encoding schemes, are not sufficient for universal quantum computation. In fact, the Gottesman-Knill theorem [42] gives us a constructive way to efficiently simulate Clifford circuits purely classically.

However, they can be supplemented with a non-Clifford gate using measurement based protocols that only involves Clifford operations [6,7] and noisy ancilla states, thus rendering the computation universal. These procedures require distilling “nonstabilizerness”, or magic, into a usable form. Therefore, magic, being a resource [43] in such fault-tolerant computation schemes, aims to quantify the degree to which states fail to be captured by stabilizer states. There are many magic measures. For example, the most straightforward definition is the minimum distance between a state of interest ρ and the set of stabilizer states,

$$D(\rho) = \min_{\sigma \in \text{STAB}} \|\rho - \sigma\|, \quad (2.1)$$

where STAB denotes the set of stabilizer states. However, this measure is difficult to compute practically. A number of computable measures have also been proposed [43–46].

In this work, we will use one such measure designed for qubit systems called the robustness of magic (ROM) [44],

defined for an arbitrary density matrix ρ ,

$$\mathcal{R}(\rho) = \min \left\{ |x|_1 : \rho = \sum_i x_i s_i, x_i \in \mathbb{R} \right\}, \quad (2.2)$$

where the s_i correspond to density operators of stabilizer states. Note that the coefficients can be negative, allowing us to express arbitrary states in this way. This quantity is lower bounded by 1 in order to have a normalized density matrix. If ρ is a stabilizer state, then there will simply be a single nonzero coefficient.

As ROM is unity for all stabilizer states, here we use $\ln(\mathcal{R})$, which we call LROM, to avoid the offset for stabilizer states and for similarities with definitions like mana [43]. However, unlike mana, which is additive for product of magic states, LROM is, in general, subadditive:

$$\begin{aligned} \mathcal{R}(\rho_1 \otimes \rho_2) &\leq \mathcal{R}(\rho_1)\mathcal{R}(\rho_2) \\ \Rightarrow \ln[\mathcal{R}(\rho_1 \otimes \rho_2)] &\leq \ln \mathcal{R}(\rho_1) + \ln \mathcal{R}(\rho_2). \end{aligned} \quad (2.3)$$

To distinguish local from nonlocal magic, we will compute magic for different subsystems in a single state. If, for instance,

$$\ln \mathcal{R}(\rho_{12}) > \ln \mathcal{R}(\rho_1) + \ln \mathcal{R}(\rho_2), \quad (2.4)$$

we will then conclude that there is magic stored nonlocally in the joint system ρ_{12} which is not found in each of the individual subsystems.

B. Bravyi-Kitaev magic distillation

Here we review the Bravyi-Kitaev (BK) MSD protocol for distilling a particular magic state, the T state. Like in the original work, we assume that stabilizer operations are easy. Therefore, T -type magic can be supplied by any state which obtained by a stabilizer operation acting on a specific T state, which we call $|T_0\rangle$. Those familiar with the Bravyi-Kitaev protocol can mostly skim this section, though we will establish some notation that will be used later in future sections.

The $|T_0\rangle$ state is the following qubit state:

$$|T_0\rangle = \cos(\theta_T)|0\rangle + e^{i\pi/4} \sin(\theta_T)|1\rangle, \quad (2.5)$$

where

$$\theta_T = \frac{1}{2} \cos^{-1} \left(\frac{1}{\sqrt{3}} \right).$$

It can also be advantageous to write $|T_0\rangle$ in terms of its density matrix.

$$|T_0\rangle\langle T_0| = \frac{1}{2} \left(I + \frac{1}{\sqrt{3}}(X + Y + Z) \right). \quad (2.6)$$

where X , Y , and Z are the single-qubit Pauli matrices. The density matrix makes manifest that one can also describe the state by its polarization vector $\vec{r} = \frac{1}{\sqrt{3}}(1, 1, 1)$ on the Bloch sphere. Similarly, one can write the $|T_1\rangle$ state as

$$|T_1\rangle\langle T_1| = \frac{1}{2} \left(I - \frac{1}{\sqrt{3}}(X + Y + Z) \right). \quad (2.7)$$

From the polarization vector, one can see that $|T_0\rangle$ points in the direction normal to one of the triangular faces of the stabilizer octahedron. By the symmetries of the stabilizer octahedron, there are eight states which serve the same magical purpose, all related by single-qubit Clifford operations. Thus

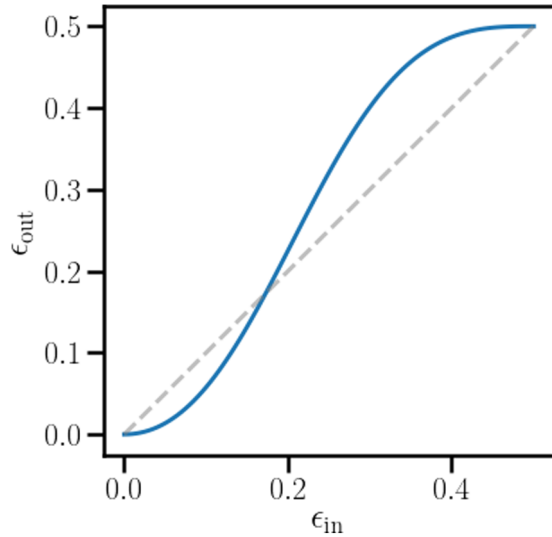


FIG. 1. The output fidelity (solid blue) as a function of input fidelity after a single round of Bravyi-Kitaev magic distillation. For reference, the dashed gray line indicates the identity channel $\epsilon_{\text{in}} = \epsilon_{\text{out}}$. The crossover point is $\epsilon^* \approx 0.173$. If the input states are not sufficiently close to a T state, then they will limit to the maximally mixed state.

successful T distillation occurs whenever any of the eight states are produced, of which $|T_0\rangle$ and $|T_1\rangle$ are two. Likewise, a T state may refer to any of these states, and we define the T fidelity to be the maximum fidelity of a state with any of the T states,

$$F_T(\rho) = \max_{U \in \mathcal{C}^{(2)}} \{F(\rho, U|T_0\rangle\langle T_0|U^\dagger)\}. \quad (2.8)$$

Here we use $\mathcal{C}^{(2)}$ to denote the Clifford group over a single qubit.

The Bravyi-Kitaev protocol for T -state distillation involves a recursive subroutine based on the $[[5,1,3]]$ code [47] whose stabilizer group is

$$\mathcal{S} = \langle XZZXI, IXZZX, XIXZZ, ZXIXZ \rangle. \quad (2.9)$$

It distills T states because the code admits a transversal implementation of the Clifford gate $B = \exp(i\pi/4)SH$ for which $|T\rangle$ is an eigenstate. As usual, S, H are the single qubit $\pi/2$ -phase gate and the Hadamard gate respectively.

Given five copies of an approximate T state of the form

$$\rho_{\text{in}} = (1 - \epsilon)|T_0\rangle\langle T_0| + \epsilon|T_1\rangle\langle T_1|, \quad (2.10)$$

the MSD protocol involves measuring the generators of \mathcal{S} and post-selecting the trivial syndrome, effectively projecting the input state onto the code subspace. If a nontrivial syndrome is measured, the state is simply discarded and the protocol is restarted. The decoding circuit is then applied to return a single qubit state, which iteratively approaches a pure T state, provided the fidelity of ρ_{in} with any T state is sufficiently high.¹ For every iteration of this procedure, one obtains noisy

¹Equivalently, it is the same to first apply the decoding circuit then measure the disentangled syndrome qubits separately [48].

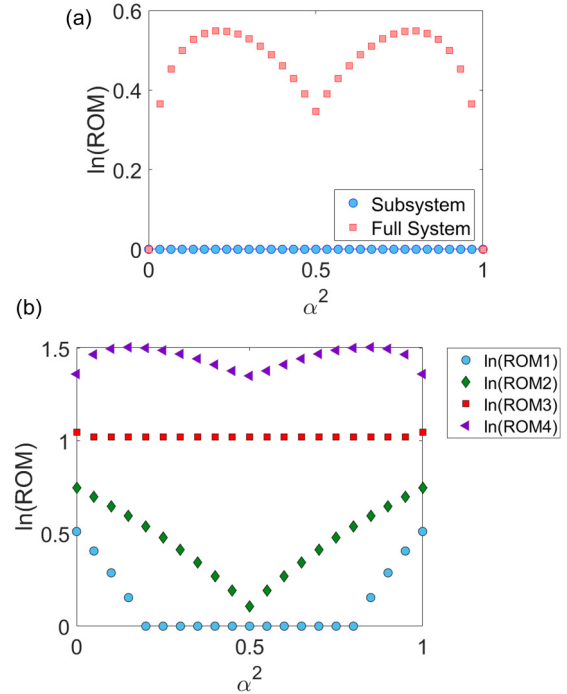


FIG. 2. (a) Magic distribution of the phase-GHZ state with phase $\phi = \pi/4$. For PGHZ, all subsystems have the same form of reduced density matrix. (b) Magic of various subsystems for the four-qubit GHZ- T state as a function of α^2 .

ancilla with a different fidelity. We plot the input and output fidelities as a result of this procedure in Fig. 1.

It is worth noting that the input state, which is a tensor product of one qubit states, is certainly not in the code subspace. Because there is only a single logical qubit, one can decompose the projected state in the basis of the encoded magic states $|T_0^L\rangle$ and $|T_1^L\rangle$. The crux of the analysis lies in showing that, for sufficiently small ϵ , the T fidelity increases. If for any $\epsilon < \epsilon^*$ such that the protocol always increases the T fidelity of the input state, then $1 - \epsilon^*$ is known as the distillation threshold.

When it comes to the efficiency of the procedure in creating magic states, there are two factors that determine the resource estimate. Assuming there is a target T fidelity, one can use the curve in Fig. 1 to estimate how many rounds of distillation are required starting from an initial pool of noisy ancilla. The second quantity of practical importance is the success probability for measuring trivial syndrome. By success probability we mean the probability of measuring the trivial syndrome corresponding to a single iteration of the distillation, as opposed to producing an approximate T state with the desired final fidelity after multiple rounds.

For input states of the form (2.10), the success probability depends on ϵ as well. As seen in Fig. 3, this is upper bounded by $1/6$, meaning every round of distillation in expectation requires at least 30 approximately magical qubits. Since it is assumed that all five input qubits are the same, one actually needs access to an exponential number of noisy ancilla due to the recursive nature of the protocol.

The utility of T states was also discussed in the same paper by Bravyi and Kitaev. They showed explicitly how to enact

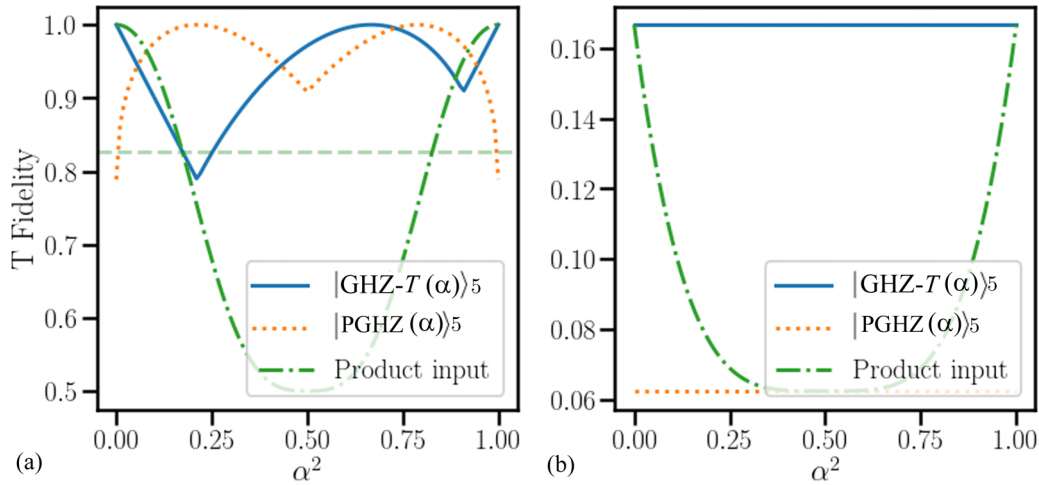


FIG. 3. With our choice of simple entangled states, we apply the BK protocol and measure the magic fidelity of the resulting qubit in (a). For comparison, we also compute it for the product states considered in the original work. Notably, the output fidelity is above threshold across a wide range of $\alpha^2 \sim 1 - \epsilon$. The output of this round can then be recursively iterated. The dashed green line shows the distillable threshold for states of the form (2.10). For the other states, they reach a pure T state except for a few specific values of α . This more lenient threshold is not a contradiction since the output density matrix of this round is not of the same form. In (b), we show the probability to measure the trivial syndrome. To actually produce a T state, one needs the procedure to both converge to a T state and measure the trivial syndrome.

a non-Clifford gate with access to T states and only Clifford operations. The fact that the same state was the fixed point of the distillation procedure and enables Clifford operations to enact universal quantum computation was the reason for calling these states “magic states.”

III. MAGIC DISTILLATION BEYOND PRODUCT STATES

In this section, we investigate whether existing MSD procedure can distill magic from nonproduct states. Indeed, the conventional input for such protocols $\rho_{in}^{\otimes n}$ is a product state. Magic is localized to each bit and there is clearly no magic hidden in the quantum correlations. However, one might ask whether other forms of multiqubit magic states can also be used to distill desired magic states as long as certain conditions are satisfied. In particular, can the distillation procedure distill magic from states where the state has entanglement or correlation such that magic is nonlocally distributed, i.e., magic of any single qubit is small whereas that of a larger subsystem is nontrivial? For example, such states can exist in the ground state of quantum many-body systems [34,35]. To this aim, we construct a few informative examples below each with distinct but carefully designed magic distributions and answer the above question in the affirmative by testing them using the BK protocol. For all of the distillation procedures below, we only use the entangled states as inputs for the first iteration. The ensuing iterations work under the conventional assumptions where multiple tensor copies of the outputs from earlier iterations are used.

A. Phase-GHZ and GHZ- T states

We begin with a few structurally simple states to build intuition. Consider Greenberger-Horne-Zeilinger (GHZ) states in the computational basis with a phase:

$$|\text{PGHZ}(\alpha)\rangle_n = \alpha|0\rangle^{\otimes n} + e^{i\phi}\beta|1\rangle^{\otimes n}. \quad (3.1)$$

For instance, one can choose $\alpha \in [0, 1]$, which sets the relative weighting of the superposition. By normalization, we choose $\beta = \sqrt{1 - \alpha^2} \in \mathbb{R}$. For extreme values of α/β , this becomes arbitrarily close to a simple product state, allowing us to “tune” the presence of magic. The specific magic distribution is shown in Fig. 2(a).

This state provides a sharp contrast with the conventional input states of MSD: no proper subsystem is magical as they are all density matrices diagonal in the computational basis. However, the overall state clearly is magical because one can turn this state into the product of $|0\rangle$'s and a single qubit magic state $\alpha|0\rangle + e^{i\phi}\beta|1\rangle$ by applying a series of Clifford gates.

This state is distillable using BK (Fig. 3) for most values of α because the output is above the distillation threshold (dashed line). Although BK is suboptimal for distilling magic from such kind of states, it clearly demonstrates that nonlocal magic remains distillable using existing protocols.

Other than the conventional product input states which have magic strictly localized to each qubit and the phase-GHZ state above where magic is strictly global, one can also construct states that have magic at different scales. Consider a state that takes the following form on n qubits:²

$$|\text{GHZ-}T(\alpha)\rangle_n = \alpha|T_0\rangle^{\otimes n} + e^{i\phi}\beta|T_1\rangle^{\otimes n}. \quad (3.2)$$

Such a state is chosen precisely because it is a combination of the noisy ancilla input and the phase-GHZ state above. While each one-qubit reduced density matrix mimics the conventional noisy ancilla input that shows up in the protocol (e.g., $\epsilon = \beta^2$), the overall state is also similar to the phase-GHZ state where there is additional magic globally. Thus, for α or β small, magic is locally distributed. However, for other choices

²While we do not use the degree of freedom of the relative phase in this work, it is one that's available to us and others for future work.

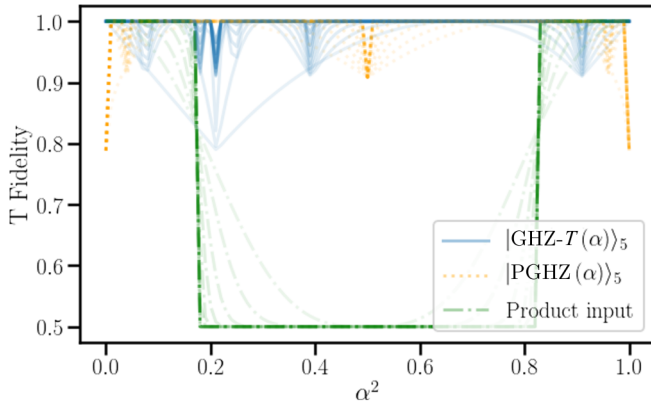


FIG. 4. Multiple iterations of the BK protocol for simple input states. Over a wide range, our choice of toy entangled states are distillable. Original product input states are limited to the tail ends where $\alpha^2 < \epsilon_*$ or $\alpha^2 > 1 - \epsilon_*$.

of α, β the state can pick up a nontrivial contribution from nonlocal magic in the n -qubit GHZ state. One can see that magic [Fig. 2(b)] on small subsystems of one or two qubits has a distribution similar to that of the conventional input states. However, as we go to larger subsystems, there is also more nonlocal magic which adds to the total global magic available in the state.

Magic in such states are mostly distillable. See Fig. 3(a) for the resulting magic fidelity after a single round and Fig. 4. for the result after multiple iterations. However, the dips in the distillability plot now no longer coincide with the locations where there is less total magic, which was the case for phase-GHZ states.

We can ask whether how global magic helps with distillation in these examples. Other than the clear improvement in distillability in the region where $\beta^2 = \epsilon \in [\epsilon^*, 1 - \epsilon^*]$, where the conventional input actually leads to lower magic fidelity, there is also improvement in the form of success probability. Since the BK protocol relies on measurement of the trivial syndrome, one must factor in the probability this occurs. In Fig. 3(b), we show that GHZ- T states improve this probability. Indeed, the GHZ- T state, which has single-qubit states identical to conventional noisy ancilla input but nonzero nonlocal magic, retains a relatively high success probability for all values of α , which is distinct from the product state counterpart.

B. Squeezed spin states from noisy ancillae

The above examples are conceptually clean and easy to understand, but may be hard to prepare in the laboratory. For entangled input states that are slightly more realistic, we consider initially states that are product stabilizer states that suffer from single-qubit coherent noise. We then perform a global entangling unitary usually used in spin squeezing procedures [49] on such states and examine how it improves distillation outcome. Spin squeezed states have been implemented in atomic cavities going back a couple of decades, primarily with application to quantum metrology and detecting quantum entanglement [50–55].

The initial ancilla states before squeezing are spins that are parallel to, say, the x axis, but have small misalignments across the spins. More explicitly,

$$|\psi_{\text{ini}}\rangle = \bigotimes_{i=1}^5 |\theta_i\rangle, \quad |\theta_i\rangle = \cos \theta_i |0\rangle + \sin \theta_i |1\rangle, \quad (3.3)$$

where the orientation of each spin θ_i can fluctuate to simulate inhomogeneity of the initial spin alignment. This is modeled by choosing each $\theta_i \in [\bar{\theta}_i - \theta_{\text{max}}, \bar{\theta}_i + \theta_{\text{max}}]$ randomly from a uniform distribution. We take the means $\bar{\theta}_i$ to be equal for all i . For example, $\bar{\theta}_i = \pi/4$ creates a product state that is approximately $|++++\rangle$ but with small misalignment across the spins. Despite the small amount of local magic introduced to $|\psi_{\text{ini}}\rangle$ through the spin misalignments, such states remain mostly undistillable, especially for θ_{max} small.

To define the unitary squeezing process, consider a total spin-5/2 system consisting of five qubits. It is known that a pure product state of qubits is not a squeezed state [49,55], and squeezing introduces entanglement among the qubits. For example,

$$|++++\rangle = 2^{5/2} \sum_{k=0}^5 \sqrt{\binom{5}{k}} \left| S = \frac{5}{2}, S_z = \frac{5}{2} - k \right\rangle \quad (3.4)$$

Squeezing can then be performed by considering some unitary rotation on the $S = 5/2$ submanifold. The initial spin misalignments sometimes introduce components that are outside the $S = 5/2$ submanifold, and the unitary mapping over the five qubits leaves these components unchanged. We can use the one-axis twisting method [49] with unitary $U(t)$ to generate a number of squeezed states $|\psi_{\text{ri}}\rangle$:

$$U(t) = \exp[-itS_z^2] \oplus I, \quad |\psi_{\text{ri}}(t)\rangle = U(t)|\psi_{\text{ini}}\rangle. \quad (3.5)$$

Note that although $U(t)$ is not a Clifford unitary, there is also no need for it to be fault-tolerant or extremely precise, as a range of different t 's can all yield similar outcomes.

For small t , the action of $U(t)$ introduces a small amount of mostly nonlocal magic and entanglement to the initial state. See Fig. 5(b) for results when $\langle \theta_i \rangle = \pi/4$. Surprisingly, the previously undistillable initial states are now mostly distillable by applying $U(t)$ [Fig. 5(a)]. Here cost is defined as the average number of copies of the same state needed to distill a single copy of the T state with a reasonably high fidelity $[F_T(\rho) \geq 0.97]$ for the plots. If the resulting output does not exceed the prescribed fidelity cutoff after 15 iterations, we deem the state undistillable and it is assigned cost -1 to differentiate from the rest of the samples. Heuristically, we can also see spin squeezing as reducing what is otherwise an infinite distillation cost to a finite number as none of the initial input states were distillable.

This is another clear demonstration that entangled states generated in a more practical laboratory setting [50–53] can help enhance the outcome of magic state distillation. While this is encouraging, squeezing does not always improve distillation outcomes. This is particularly visible when the input states are already T states with relatively high fidelity because they act like a source of correlated noise. We further discuss the role played by spin squeezing in Appendix B. We wish to point out that it is difficult to directly compare the

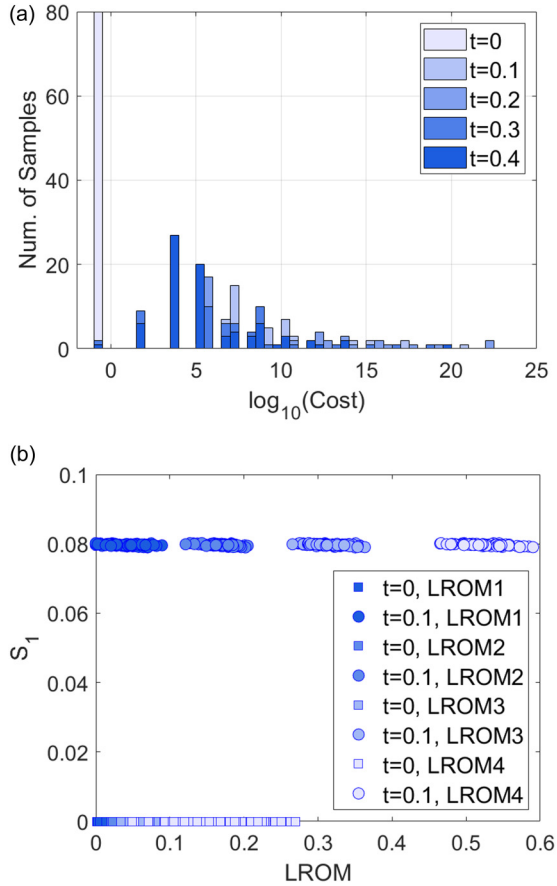


FIG. 5. (a) Figure of distillability of states with ($t \neq 0$) vs without ($t = 0$) squeezing ($\theta_{\max} = 0.05$). States without squeezing (blue) are undistillable and are assigned cost -1 . (b) Single-site entanglement and magic of various subsystems of squeezed (colored disks) vs unsqueezed states (colored squares) with $\bar{\theta}_i = \pi/4$.

cost of a procedure with spin squeezing with the cost from conventional distillation procedures. This is because their inputs are in totally different regimes: the cost in the original BK protocol is computed assuming product of noisy ancilla states above distillation threshold, whereas the advantage of spin squeezing is to take states that are below the distillation threshold, e.g., very close to stabilizer states, and make them distillable. For this reason, the starting point for the procedures is hard to standardize between the two approaches. Taking a step back, we would like to emphasize that the lesson learned from spin squeezing is that a totally different class of states, even without magic, from the original noisy ancilla proposed can be made distillable. For those interested in making magic factories, it broadens the horizon of possible inputs and encourages us to look for other experimentally viable entangled states.

IV. UNDERSTANDING DISTILLABILITY

In this section, we examine the underlying $[[5,1,3]]$ code that powers the BK distillation procedure to understand properties of states that contain distillable magic. In doing so, we present a few key observations. First, using elementary ideas from quantum error correction, we can deduce the form of

nonlocal magic content for the ideal input state. We then investigate these intuitions by generating random BK-distillable states whose success probability is lower bounded by that of product input states. Studying their entanglement and magic distribution properties tells us that the typical product ansatz is highly fine-tuned. Second, we can explain explicitly why the total magic in a state does not correlate with the distillable magic for this protocol. We expect the lessons here to generalize appropriately for any magic distillation procedure which relies on a quantum error correcting code.

As mentioned previously, the Bravyi-Kitaev distillation procedure (decoding followed by post-selecting the trivial syndrome) can be represented as a linear map $M : \mathcal{H}_{\text{in}} \rightarrow \mathcal{H}_{\text{out}}$, where $\mathcal{H}_{\text{in}}, \mathcal{H}_{\text{out}}$ are 32- and 2-dimensional Hilbert spaces, respectively. Then for each normalized five-qubit input $|\psi_{\text{in}}\rangle \in \mathcal{H}_{\text{in}}$, we can obtain a single-qubit output $|\psi_{\text{out}}\rangle \in \mathcal{H}_{\text{out}}$ such that

$$\lambda|\psi_{\text{out}}\rangle = M|\psi_{\text{in}}\rangle. \quad (4.1)$$

As a portion of $|\psi_{\text{in}}\rangle$ may not lie in the code subspace, the probability of success $|\lambda|^2$, i.e., measuring a trivial syndrome, satisfies $0 \leq |\lambda| \leq 1$. It is clear that states with more overlap with the code subspace have higher success probability.

Working in the basis of the code subspace, any input state with unit success probability can be written as

$$|\psi_{\text{in}}\rangle = a|T_0^L\rangle + b|T_1^L\rangle, \quad (4.2)$$

where the size of a will determine the output state fidelity. This works because the perfect code encodes a single qubit.

It is immediately clear that states close to the encoded T states will have both high success probability and good T fidelity. Furthermore, because the code corrects two qubit erasure errors, any encoded information must be found in three or more qubit subsystems. Therefore, for states with high success rate, i.e., large overlap with the code subspace, the amount of magic found in 3 or more qubit subsystems should positively correlate with the output fidelity. On the other hand, such states will have very little magic in one or two qubit subsystems.

However, when a state does not overlap significantly with the code subspace, namely $|\lambda|$ small, the connection between the amount of magic, its distribution, and output fidelity is no longer clear.

To get an idea of a typical distillable state, we generate random states uniformly in the space of states where their output fidelity is above the BK distillation threshold and $|\lambda| > 0.16$ is reasonably large. As a reference, the success probability for product input states close to T states is ~ 0.167 (see Fig. 3).

We see that the typical distillable states are not only entangled, but also have nonlocal magic (Fig. 6). As we see, any subsystem is close to being maximally mixed while magic localized to any single qubit is virtually nonexistent. This is in sharp contrast with the conventional input states which have neither. Therefore, this observation indicates that having many-body quantum states beyond the typical product input states can improve the magic distillation outcomes.

However, unlike the conventional input states, there is no obvious correlation between the total amount of magic or entanglement a state has and the distillation outcome. In fact, if anything, too much magic can negatively impact distillability in terms of the success probability. We can try to understand this observation from two limits.

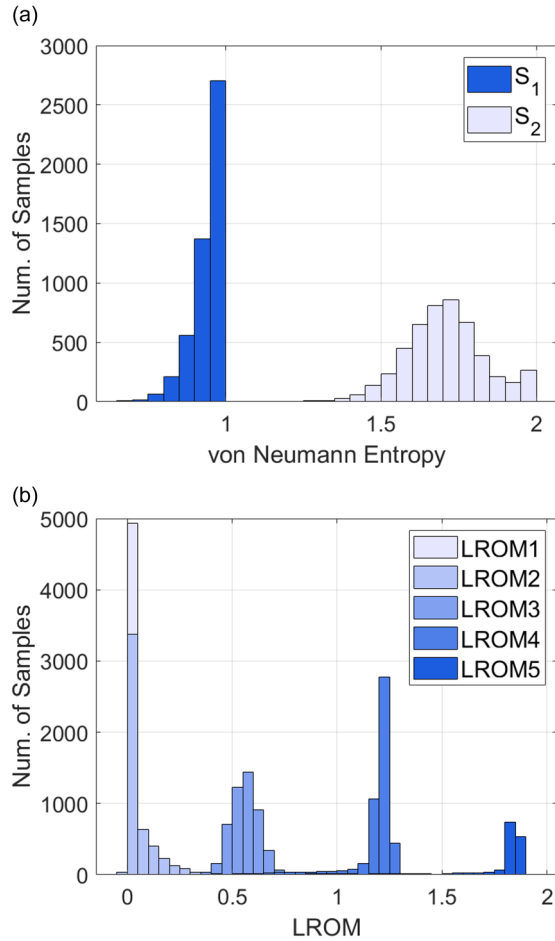


FIG. 6. (a) Distribution of von Neumann entropies for single- and two-qubit subsystems. (b) LROM distribution in the random BK-distillable states.

In the limit where the state is perturbatively close to the encoded T state, then having a state whose magic or entanglement pattern that deviates from the state that has the single best distillable outcome will obviously result in a worse distillation outcome. The maximum amount of magic for a state in the code subspace is upper bounded by that of a single T state (LROM ~ 0.55). If the input state has more magic than this, then it is necessarily out of the code subspace thus resulting in a lower success probability (Fig. 7). If, on the other hand, the total magic is less than the upper bound, then it can have a large overlap with the code subspace. In that case, the success probability is close to 1, but its output fidelity must suffer for being farther from the encoded T state. There is a direct correlation between the amount of magic and output fidelity. This can be seen in Fig. 8, but is less pronounced in Fig. 7. Interestingly, it is also difficult to find a distillable state that has less total magic than that of a T state but also small overlap with the code subspace. This is likely related to the fact that (Haar) random states are magical [38].³

³Interestingly, LROM of a larger subsystem has such a smaller variance compared to that of a smaller system. This is also quali-

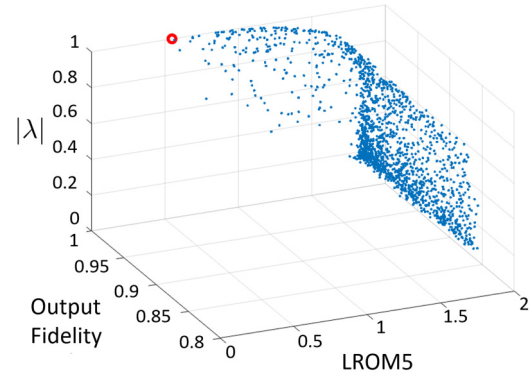


FIG. 7. LROM5 of random states (blue) against output fidelity and success probability. The red circle denotes the location of the encoded T state.

In the limit where a state has small overlap with the code subspace ($|\lambda| \lesssim 0.4$), the previous arguments no longer apply. Instead, there is no clear correlation between output fidelity, success probability, and the amount of magic.

One can also compute the average cost of distilling magic from these typical states. Again, there is no obvious correlation between the total magic of a state and the total cost for generating a magic state with desired T fidelity $F_T(\rho) > 0.999$.

However, there are states with magic lower than that of a typical state that have slightly lower cost, as shown in the thin narrow bands stretching to the left of the cluster (Fig. 9). These are precisely the states that have higher success probabilities which are closer to the encoded T states. Curiously, these states concentrate on the ridges but are not found anywhere in between, unlike the typical states that contain more magic.

tatively consistent with results from Haar random states [38] where the variance of magic scales roughly as $\sim e^{-L}$ where L is the number of sites.

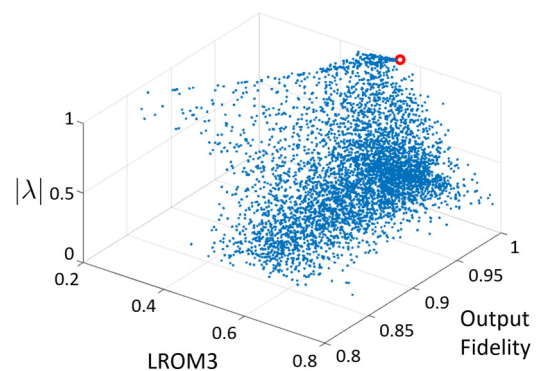


FIG. 8. LROM3 of random states (blue) against output fidelity and success probability. The red circle denotes the location of the encoded T state. On the plane $|\lambda| = 1$, there is clear correlation between LROM and output fidelity.

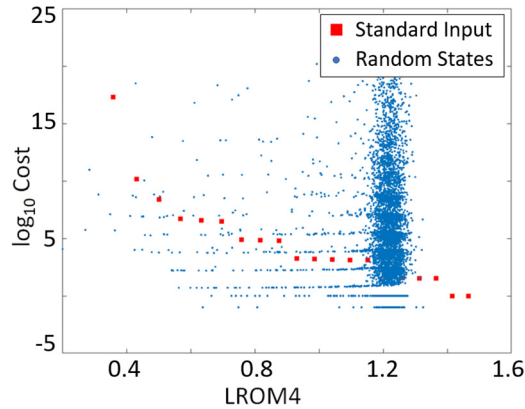


FIG. 9. Plotting LROM4 and cost for random states (blue) and conventional inputs (red). Cost is set to -1 if the state does not exceed the prescribed fidelity $F_T(\rho) > 0.999$ within 15 iterations of the protocol.

V. DISCUSSION

In this work, we have examined how entanglement and nonlocal magic can impact the outcome of magic state distillation. Using the BK protocol on five qubits, we establish that nonlocal magic is indeed distillable. Furthermore, numerical experiments indicate that nonlocal magic in these entangled states can also “assist” the usual magic distillation process by lowering the cost of overall distillation. This is outlined conceptually by studying the GHZ- T and GHZ phase states. More practically, we have also constructed a spin-squeezing-assisted procedure for noisy ancilla states. It is shown that certain squeezing operations indeed render nondistillable states distillable, which may be more relevant in an experimental setting.

Although the overall impact of many-body magic is still largely unclear in the context of distillation, we build up some generalizable intuition using the five-qubit code and argue that, for the existing distillation protocols based on quantum error correction codes, a typical distillable state should be entangled.

Because of the common assumptions behind magic state distillation, one might have suspected that entanglement generally introduces a source of correlated noise, thereby reducing the output fidelity and success rate of magic distillations. However, this expectation is likely a streetlight effect of only searching perturbatively near the conventional product input states. While it is a valid expectation in certain cases (e.g., Fig. 13), it is abundantly clear that, by analyzing the entanglement structure and magic distribution of the encoded T state, a typical distillable state is anything but a product state with local magic.

One might also suspect that a larger amount of total magic would generally lead to better distillation outcomes. This is somewhat suggestive from Figs. 2(a) and 4 for phase-GHZ states. However, this correlation is only manifest when the input lies predominantly in the code subspace. Analysis in Sec. IV indicates that this intuition has limited applicability when the overlap between the input and the code subspace is small. There it is unclear what properties would positively correlate with distillability.

Since our work suggests that entangled states may assist magic distillations, it opens up a number of directions in the area of many-body magic [34–36,38]. Thus far we have only focused on examples and numerical analysis; however, a more systematic approach is needed to understand many-body magic distillability that is not protocol specific. Generally, we want to understand the features in the distillation protocol and those of the many-body states that will lead to better distillation outcomes. In particular, it opens up the question of what a “typical” distillable magic state should look like if one looks beyond product of identical states. It is also unclear whether existing protocols are optimal for distilling many-body magic, as the input states are drastically different. For example, while it is well known that bound magic states exist [56] assuming identical inputs, it is not clear to what extent the same conclusion applies when one also considers more general input states. We would also like to understand what kind of protocols are near optimal in distilling magic from condensed matter systems such as the low energy states of a spin chain where magic is abundant.

It is possible that holographic quantum error correction codes may also be useful in this regard for distilling multiscale nonlocal magic from conformal field theories (CFTs) due to its multiscale, self-similar structure. It was pointed out recently [57] that holographic codes with good complementary recovery properties have difficulties implementing transversal non-Clifford gates. Nevertheless, it is still entirely possible to construct holographic codes in general that do have transversal T gates. For instance, this can be done by using codes with transversal non-Clifford gates [2,58] such as the $[[15,1,3]]$ Calderbank-Shor-Steane (CSS) code [59,60] as the base tensor, which supports a transversal logical \bar{T} gate. Using the general methodology outlined in [61] (and more comprehensively in [62]) for building tensor networks on two-dimensional hyperbolic space with regular tessellations, one can produce a holographic code constructed using the $\{15, q \geq 4\}$ tiling. This results in an $[[n, k]]$ CSS code that admits a transversal $\bar{T}^{\otimes k}$ gate.⁴ The same methodology also applies to more general $[[2^{n-1}, 1, 3]]$ punctured Reed-Muller codes [63] in a $\{2^{n-1}, q \geq 4\}$ tessellation. The resulting stabilizer code would again admit a transversal non-Clifford gate. It should also be noted that transversal non-Clifford gates are not always necessary for distillation. Indeed, the five-qubit code does not admit a transversal T gate; however, the transversal B gate enables distillation of T states. A holographic code that serves a similar purpose is the $[[n, k]]$ stabilizer code known as the HaPPY pentagon code [41]. There the logical $\bar{B}^{\otimes k}$ is transversal and a protocol similar to BK may be sufficient for T state distillation.

ACKNOWLEDGMENTS

We thank Greg Bentsen for the stimulating discussions on the experimental feasibility of creating entangled states and the suggestion to look at spin squeezing. C.C. acknowledges the support by the U.S. Department of Defense and

⁴Note that the tensors or codes used to build the holographic code can be the same up to local Clifford equivalences.

NIST through the Hartree Postdoctoral Fellowship at QuICS, by the Simons Foundation as part of the It From Qubit Collaboration, and by the DOE Office of Science, Office of High Energy Physics, through Grant No. DE-SC0019380. N.B. is supported by the Department of Energy under Grant No. DE-SC0019380, by the Computational Science Initiative at Brookhaven National Laboratory, and by the U.S. Department of Energy QuantISED Quantum Telescope award. V.P.S. is supported in part by the Berkeley Center for Theoretical Physics, by the National Science Foundation (Award No. PHY-1521446), and by the U.S. Department of Energy under Contract No. DE-AC02-05CH11231 and Award No. DE-SC0019380. V.P.S. gratefully acknowledges support by the NSF Graduate Research Fellowship Program under Grant No. DGE 1752814.

APPENDIX A: DISTILLABILITY OF VARIOUS PHASE-GHZ AND GHZ- T STATES

In this Appendix we examine the distillability of states similar to those presented in Sec. III A, the phase-GHZ and GHZ- T states. As a reminder, these were n -qubit states that took the following form:

$$\begin{aligned} |\text{PGHZ}(\alpha)\rangle_n &= \alpha|0\rangle^{\otimes n} + e^{i\phi}\beta|1\rangle^{\otimes n}, \\ |\text{GHZ-}T(\alpha)\rangle_n &= \alpha|T_0\rangle^{\otimes n} + e^{i\phi}\beta|T_1\rangle^{\otimes n}. \end{aligned} \quad (\text{A1})$$

Because the Bravyi-Kitaev protocol takes as input a five-qubit state, it was a natural choice to pick $n = 5$. Not only does this make each of the reduced density matrices the same, but the input state is symmetric between the five qubits. Here, we now consider a more broad construction where we make a five-qubit state out of a combination of smaller $|\text{PGHZ}\rangle_n(|\text{GHZ-}T\rangle_n)$ states. This may lead to easier experimental implementation if it is much easier to generate, say, $|\text{PGHZ}\rangle_2$ and $|\text{PGHZ}\rangle_3$ than $|\text{PGHZ}\rangle_5$. On the theoretical side, it is interesting to ask whether the presence of more magic yields better distillation outcomes. This is because $|\text{PGHZ}\rangle_n$ has the same magic regardless of n , so $|\text{PGHZ}\rangle_2|\text{PGHZ}\rangle_3$ would have twice as much global magic as $|\text{PGHZ}\rangle_5$ for the same α .

We consider two primary variations. The first is where we make a five-qubit state out of tensor products of PGHZ states $\otimes_i |\text{PGHZ}\rangle_{k_i}$ such that $\sum_i k_i = 5$. We plot the distillation outcomes in Fig. 10 and make a few observations. The first is that adding more total magic does not seem to enhance the ability to distill. This lines up with the expectations laid out in Sec. IV. Interestingly, all of these states remained distillable for generic α .

The second variation allows for some of the qubits to be in the $|0\rangle$ state in the computational basis, a consideration for experimental setups where the $|0\rangle$ state is effectively just resetting a clean qubit. Clearly, these qubits do not add to the available magic. The results are displayed in Fig. 11. With the exception of phase-GHZ states with even numbers, these states also have a wide range of distillability.

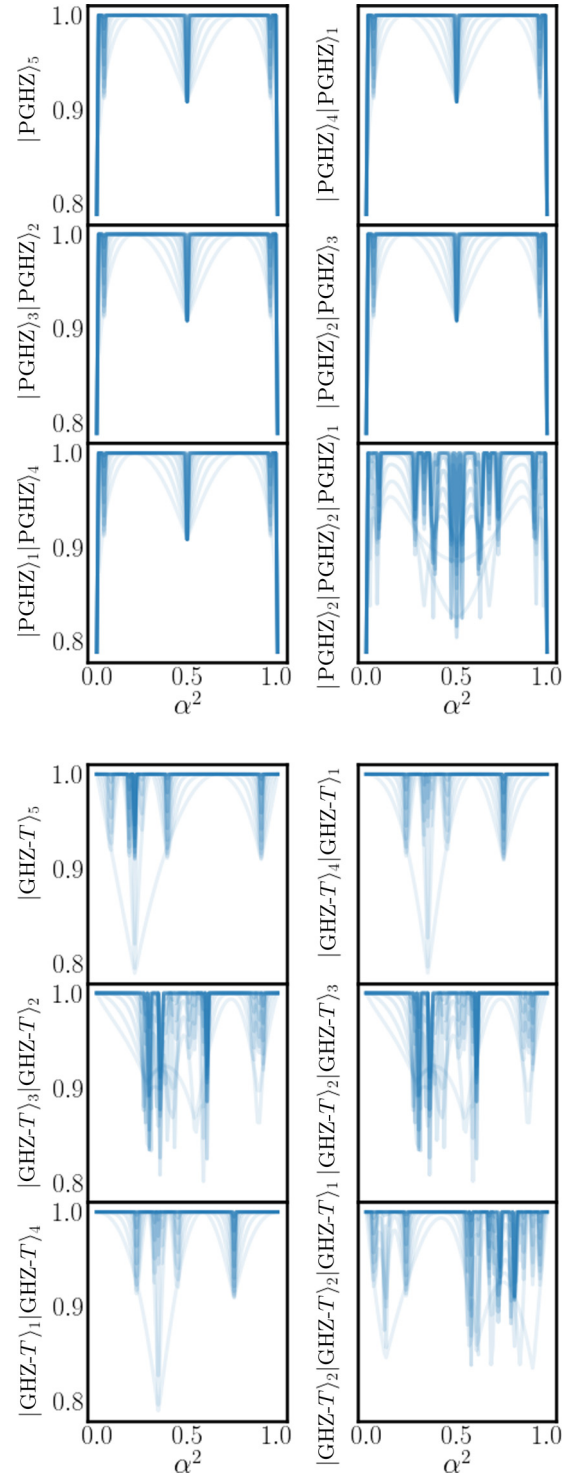


FIG. 10. Distillability of composite $|\text{PGHZ}\rangle_k$ and $|\text{GHZ-}T\rangle_k$ states, where α is taken to uniform across individual components. We plot the magic fidelity of the qubit upon a successful distillation round with darker curves corresponding to later rounds. The darkest line is the resulting T fidelity after 10 rounds. Because $|\text{PGHZ}\rangle_k$ and $|\text{GHZ-}T\rangle_k$ contain the same amount of magic for all values of k , composite five-qubit states with more individual states have more total magic in the system. We find that the presence of more total magic does not generally enhance distillability for the BK protocol.

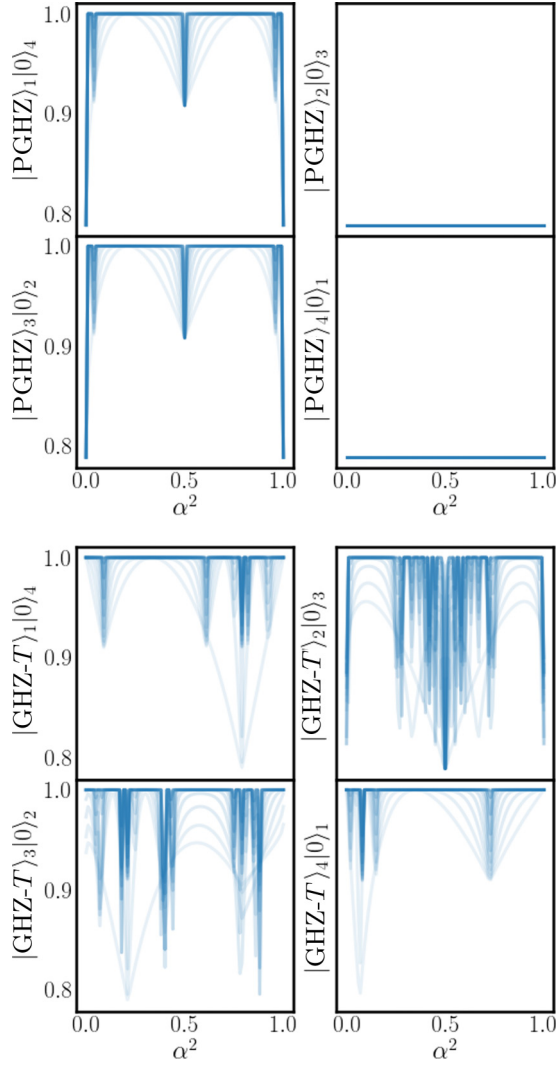


FIG. 11. Distillability of composite $|\text{PGHZ}\rangle_k$ and $|\text{GHZ-T}\rangle_k$ states, with some qubits in the $|0\rangle$ state. A notable finding is that one can get similar distillability without having to entangle the full five-qubit state.

APPENDIX B: MORE ON SPIN SQUEEZING AND DISTILLATION

Although a global entangling unitary like the one defined in Sec. III B can improve the distillation outcome, this improvement will depend on a number of factors and is not universal. Here we analyze how different initial states modified the same squeezing unitary $U(t)$ may impact the distillation outcome. Then we examine the effect of a different squeezing unitary $V(t)$. We find that improved distillation is unlikely to be connected to squeezing and overall amount of entanglement. However, its success may be related to the nonlocal magic injected during the squeezing process.

First of all, squeezing alone is not the key to improving the distillation outcome; clearly a state needs to contain enough magic to be distillable at all. Although squeezing in general can add magic to a stabilizer state, a slight squeezing of

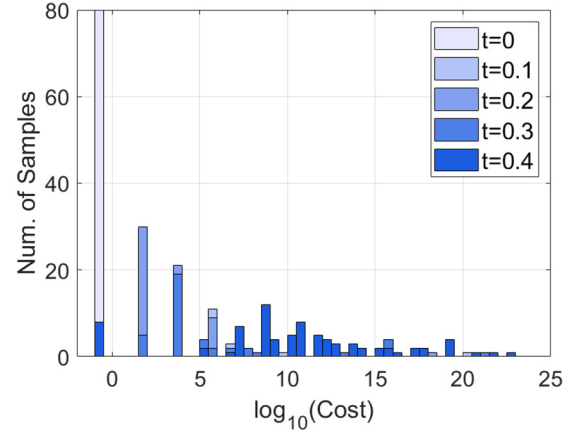


FIG. 12. BK distillation cost applied to states after one-axis twisting $|00000\rangle$ initial states with random misalignment. Here $\theta_{\max} = 0.05$.

an initial state without spin misalignment does not improve distillation outcome. Furthermore, states that are unsqueezed under the same unitary $U(t)$ [Eq. (3.5)] also see improvement in distillation. For example, distillation outcome is just as good, if not better, for initial states where $\bar{\theta}_i = 0$ (Fig. 12). However $U(t)$ does not squeeze $|00000\rangle$, which is approximately the initial state we have.

The same global unitary action $U(t)$ also need not improve distillation for other types of initial states. Sometimes it acts as coherent noise to the system, which impedes distillation. For example, consider the scenario where the individual qubit input states are sufficiently close to $|T\rangle$ such that $\bar{\beta}_i = \theta_T = \arccos(1/\sqrt{3})/2$, $\phi = \pi/4$,

$$|\tau_0^i\rangle = \cos(\beta_i)|0\rangle + \exp(i\phi)\sin(\beta_i)|1\rangle, \quad (\text{B1})$$

$$|\tau_1^i\rangle = -\sin(\beta_i)|0\rangle + \exp(i\phi)\cos(\beta_i)|1\rangle, \quad (\text{B2})$$

and the initial state is given by

$$\rho_{\text{ini}} = \bigotimes_i (p_i|\tau_0^i\rangle\langle\tau_0^i| + (1-p_i)|\tau_1^i\rangle\langle\tau_1^i|). \quad (\text{B3})$$

As usual, β_i is drawn uniformly random for an interval $[\bar{\beta}_i - \beta_{\max}, \bar{\beta}_i + \beta_{\max}]$. The probability p_i is also drawn uniformly for an interval $[\bar{p}_i - p_{\max}, \bar{p}_i + p_{\max}]$. These are precisely the target magic T states when $p_{\max}, \beta_{\max} = 0$. Then squeezing now acts as a source of noise that renders distillation less efficient (Fig. 13).

On the other hand, if the initial state is close to $|++++\rangle$ or $|00000\rangle$ but mixed, then the improvement in the distillation cost also quickly diminishes in these examples as one increases p_{\max} . For instance, consider states of the form (B3) but with $\phi = 0$, $\bar{\beta}_i = \pi/4$; the distillation cost is shown in Fig. 14 where the number of undistillable states can increase sharply even when the purity is still relatively high.

Now let us briefly examine the same process but with a different global unitary applied to the $\bar{\theta}_i = \pi/4$ initial state (3.3). Consider a different squeezing procedure using

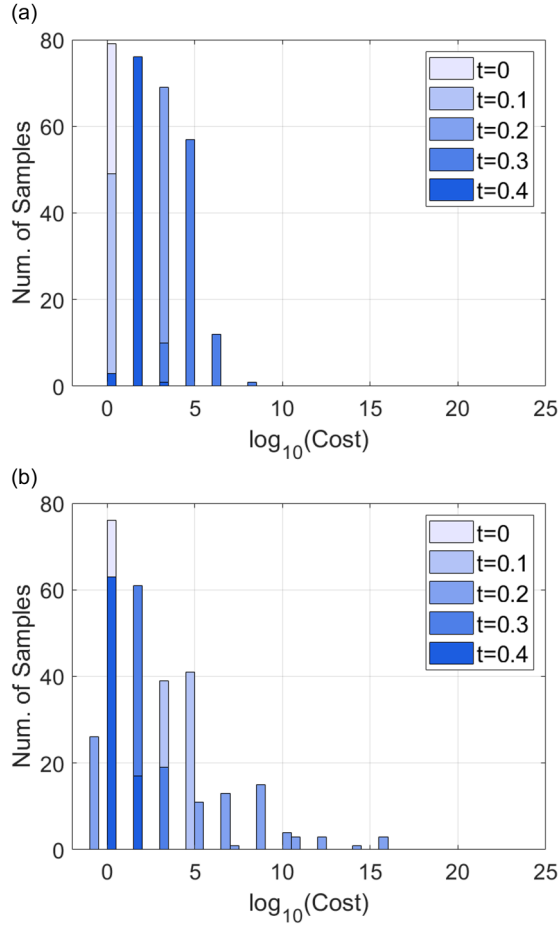


FIG. 13. (a) Squeezing the tensor product of five noisy T states via one-axis twisting. (b) Squeezing the tensor product of five noisy T states via two-axis counter-twisting. Here $\beta_{\max} = 0.05$, $p_{\max} = 0.1$ for both plots. Squeezing increases the overall cost of distillation in both cases.

two-axis counter-twisting [49] with $V(t) = \exp(-itH)$, where

$$H = \frac{1}{2i}(S_+^2 - S_-^2), \quad S_{\pm} = S_x \pm iS_y. \quad (\text{B4})$$

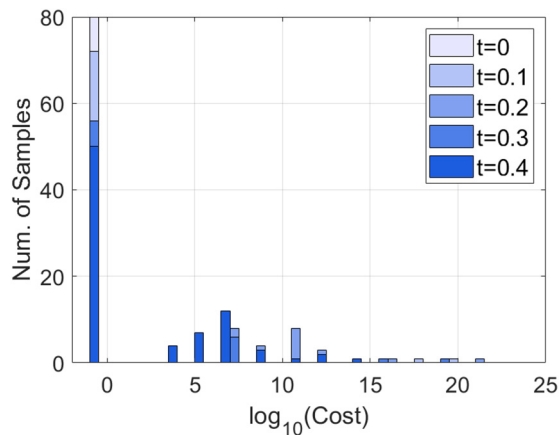


FIG. 14. One-axis twisting applied to initial mixed states that are close to a product stabilizer state. $\theta_{\max} = 0.05$ and $p_{\max} = 0.02$.

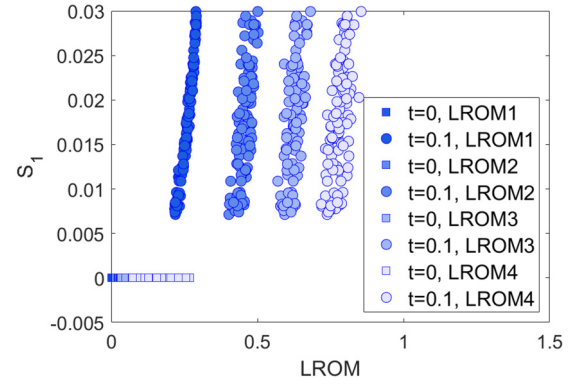


FIG. 15. LROM and single site entanglement of the state with (colored disks) and without squeezing (colored squares).

Then squeezing produces a similar level entanglement as the previous one-axis twisting procedure for similar values of t . It also increases the total magic in the state. However, no visible enhancement for the distillation can be found (Fig. 15).

The lack of improvements here may be attributed to the amount of nonlocal magic that is added to the system. Note that a pure state with nonlocal magic is most certainly entangled, but an entangled state need not contain nonlocal magic. While there is a slight addition to nonlocal magic using the one-axis twisting unitary, there is virtually no change in the two-axis counter-twisting scheme (Fig. 16). We estimate nonlocal magic using

$$\mathcal{LROM}(1:2) = \ln[\mathcal{R}(\rho_{12})] - \{\ln[\mathcal{R}(\rho_1)] + \ln[\mathcal{R}(\rho_2)]\}, \quad (\text{B5})$$

where ρ_{12} is an arbitrarily chosen two-site subsystem.

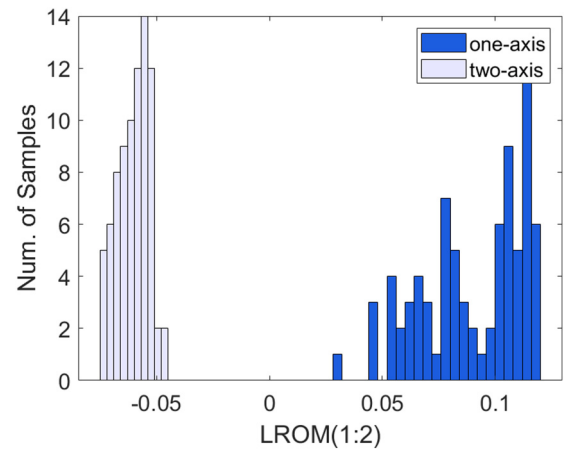


FIG. 16. Histogram contrasting two-body nonlocal magic $\mathcal{LROM}(1:2)$ after the one-axis twisting and the two-axis counter-twisting options that result in similar levels of entanglement ($S_1 \sim 0.08$ and $S_1 \sim 0.02$ respectively). Slight negativity can be attributed to the nonadditivity of LROM.

- [1] B. Eastin and E. Knill, Restrictions on Transversal Encoded Quantum Gate Sets, *Phys. Rev. Lett.* **102**, 110502 (2009).
- [2] B. Zeng, A. Cross, and I. L. Chuang, Transversality versus universality for additive quantum codes, *IEEE Trans. Inf. Theory* **57**, 6272 (2011).
- [3] S. Bravyi and R. König, Classification of Topologically Protected Gates for Local Stabilizer Codes, *Phys. Rev. Lett.* **110**, 170503 (2013).
- [4] F. Pastawski and B. Yoshida, Fault-tolerant logical gates in quantum error-correcting codes, *Phys. Rev. A* **91**, 012305 (2015).
- [5] T. Jochym-O'Connor, A. Kubica, and T. J. Yoder, Disjointness of Stabilizer Codes and Limitations on Fault-Tolerant Logical Gates, *Phys. Rev. X* **8**, 021047 (2018).
- [6] S. Bravyi and A. Kitaev, Universal quantum computation with ideal Clifford gates and noisy ancillas, *Phys. Rev. A* **71**, 022316 (2005).
- [7] E. Knill, Fault-tolerant postselected quantum computation: Schemes, [arXiv:quant-ph/0402171](https://arxiv.org/abs/quant-ph/0402171).
- [8] A. Paetznick and B. W. Reichardt, Universal Fault-Tolerant Quantum Computation with Only Transversal Gates and Error Correction, *Phys. Rev. Lett.* **111**, 090505 (2013).
- [9] T. J. Yoder, Universal fault-tolerant quantum computation with Bacon-Shor codes, [arXiv:1705.01686](https://arxiv.org/abs/1705.01686).
- [10] T. J. Yoder, R. Takagi, and I. L. Chuang, Universal Fault-Tolerant Gates on Concatenated Stabilizer Codes, *Phys. Rev. X* **6**, 031039 (2016).
- [11] T. Jochym-O'Connor and S. D. Bartlett, Stacked codes: Universal fault-tolerant quantum computation in a two-dimensional layout, *Phys. Rev. A* **93**, 022323 (2016).
- [12] S. Bravyi and A. Cross, Doubled color codes, [arXiv:1509.03239](https://arxiv.org/abs/1509.03239).
- [13] C. Jones, P. Brooks, and J. Harrington, Gauge color codes in two dimensions, *Phys. Rev. A* **93**, 052332 (2016).
- [14] B. J. Brown, A fault-tolerant non-Clifford gate for the surface code in two dimensions, *Sci. Adv.* **6**, eaay4929 (2020).
- [15] D. Gottesman and I. L. Chuang, Demonstrating the viability of universal quantum computation using teleportation and single-qubit operations, *Nature (London)* **402**, 390 (1999).
- [16] M. A. Nielsen, Quantum computation by measurement and quantum memory, *Phys. Lett. A* **308**, 96 (2003).
- [17] D. W. Leung, Two-qubit projective measurements are universal for quantum computation, [arXiv:quant-ph/0111122](https://arxiv.org/abs/quant-ph/0111122).
- [18] D. Gosset, V. Kliuchnikov, M. Mosca, and V. Russo, Quantum Inf. Comput. **14**, 1261 (2018).
- [19] M. Amy, D. Maslov, M. Mosca, and M. Roetteler, A meet-in-the-middle algorithm for fast synthesis of depth-optimal quantum circuits, *IEEE Trans. Comput. Aided Des. Integr. Circuits Syst.* **32**, 818 (2013).
- [20] Y. Nam, N. J. Ross, Yuan Su, A. M. Childs, and D. Maslov, Automated optimization of large quantum circuits with continuous parameters, *npj Quantum Inf.* **4**, 23 (2018).
- [21] L. Heyfron and E. T. Campbell, An Efficient Quantum Compiler that reduces T count, *Quantum Sci. Technol.* **4**, 015004 (2018).
- [22] Q. Wang, Ming Li, C. Monroe, and Y. Nam, Resource-optimized fermionic local-Hamiltonian simulation on quantum computer for quantum chemistry, *Quantum* **5**, 509 (2021).
- [23] H. Bombín, Gauge color codes: Optimal transversal gates and gauge fixing in topological stabilizer codes, *New J. Phys.* **17**, 083002 (2015).
- [24] A. Kubica and M. E. Beverland, Universal transversal gates with color codes: A simplified approach, *Phys. Rev. A* **91**, 032330 (2015).
- [25] M. E. Beverland, A. Kubica, and K. M. Svore, Cost of universality: A comparative study of the overhead of state distillation and code switching with color codes, *PRX Quantum* **2**, 020341 (2021).
- [26] A. Kubica, B. Yoshida, and F. Pastawski, Unfolding the color code, *New J. Phys.* **17**, 083026 (2015).
- [27] H. Bombin, Transversal gates and error propagation in 3d topological codes, [arXiv:1810.09575](https://arxiv.org/abs/1810.09575).
- [28] H. Bombin, 2d quantum computation with 3d topological codes, [arXiv:1810.09571](https://arxiv.org/abs/1810.09571).
- [29] A. M. Meier, B. Eastin, and E. Knill, *Quantum Inf. Comput.* **13**, 195 (2013).
- [30] S. Bravyi and J. Haah, Magic-state distillation with low overhead, *Phys. Rev. A* **86**, 052329 (2012).
- [31] C. Jones, Low-overhead constructions for the fault-tolerant Toffoli gate, *Phys. Rev. A* **87**, 022328 (2013).
- [32] C. Jones, Multilevel distillation of magic states for quantum computing, *Phys. Rev. A* **87**, 042305 (2013).
- [33] J. Haah, M. B. Hastings, D. Poulin, and D. Wecker, Magic state distillation with low space overhead and optimal asymptotic input count, *Quantum* **1**, 31 (2017).
- [34] S. Sarkar, C. Mukhopadhyay, and A. Bayat, Characterization of an operational quantum resource in a critical many-body system, *New J. Phys.* **22**, 083077 (2020).
- [35] C. D. White, ChunJun Cao, and B. Swingle, Conformal field theories are magical, *Phys. Rev. B* **103**, 075145 (2021).
- [36] Z.-W. Liu and A. Winter, Many-body quantum magic, [arXiv:2010.13817](https://arxiv.org/abs/2010.13817).
- [37] T. D. Ellison, K. Kato, Z.-W. Liu, and T. H. Hsieh, Symmetry-protected sign problem and magic in quantum phases of matter, *Quantum* **5**, 612 (2021).
- [38] C. D. White and J. H. Wilson, Mana in Haar-random states, [arXiv:2011.13937](https://arxiv.org/abs/2011.13937).
- [39] D. Gottesman, The Heisenberg representation of quantum computers, *Group22: Proceedings of the XXII International Colloquium on Group Theoretical Methods in Physics*, edited by S. P. Corney, R. Delbourgo, and P. D. Jarvis (International Press, MA, Cambridge, 1999), pp. 32–43.
- [40] A. Yu. Kitaev, Fault-tolerant quantum computation by anyons, *Ann. Phys. (NY)* **303**, 2 (2003).
- [41] F. Pastawski, B. Yoshida, D. Harlow, and J. Preskill, Holographic quantum error-correcting codes: Toy models for the bulk/boundary correspondence, *J. High Energy Phys.* **06** (2015) 149.
- [42] D. Gottesman, Theory of fault-tolerant quantum computation, *Phys. Rev. A* **57**, 127 (1998).
- [43] V. Veitch, S. A. Hamed Mousavian, D. Gottesman, and J. Emerson, The resource theory of stabilizer quantum computation, *New J. Phys.* **16**, 013009 (2014).
- [44] M. Howard and E. Campbell, Application of a Resource Theory for Magic States to Fault-Tolerant Quantum Computing, *Phys. Rev. Lett.* **118**, 090501 (2017).

- [45] X. Wang, M. M. Wilde, and Y. Su, Efficiently Computable Bounds for Magic State Distillation, *Phys. Rev. Lett.* **124**, 090505 (2020).
- [46] M. Beverland, E. Campbell, M. Howard, and V. Kliuchnikov, Lower bounds on the non-Clifford resources for quantum computations, *Quantum Sci. Technol.* **5**, 035009 (2020).
- [47] R. Laflamme, C. Miquel, J. P. Paz, and W. H. Zurek, Perfect Quantum Error Correcting Code, *Phys. Rev. Lett.* **77**, 198 (1996).
- [48] D. Gottesman, Stabilizer codes and quantum error correction, Ph.D. thesis, California Institute of Technology, January 1997, [arXiv:quant-ph/9705052](https://arxiv.org/abs/quant-ph/9705052).
- [49] M. Kitagawa and M. Ueda, Squeezed spin states, *Phys. Rev. A* **47**, 5138 (1993).
- [50] M. H. Schleier-Smith, I. D. Leroux, and V. Vuletić, Squeezing the collective spin of a dilute atomic ensemble by cavity feedback, *Phys. Rev. A* **81**, 021804(R) (2010).
- [51] I. D. Leroux, M. H. Schleier-Smith, and V. Vuletić, Implementation of Cavity Squeezing of a Collective Atomic Spin, *Phys. Rev. Lett.* **104**, 073602 (2010).
- [52] T. Ono, J. Sabines-Chesterking, H. Cable, J. L. O'Brien, and J. C. F. Matthews, Optical implementation of spin squeezing, *New J. Phys.* **19**, 053005 (2017).
- [53] J. Hald, J. L. Sørensen, C. Schori, and E. S. Polzik, Spin Squeezed Atoms: A Macroscopic Entangled Ensemble Created by Light, *Phys. Rev. Lett.* **83**, 1319 (1999).
- [54] R. J. Sewell, M. Koschorreck, M. Napolitano, B. Dubost, N. Behbood, and M. W. Mitchell, Magnetic Sensitivity Beyond the Projection Noise Limit by Spin Squeezing, *Phys. Rev. Lett.* **109**, 253605 (2012).
- [55] G. Tóth, C. Knapp, O. Gühne, and H. J. Briegel, Spin squeezing and entanglement, *Phys. Rev. A* **79**, 042334 (2009).
- [56] E. T. Campbell and D. E. Browne, Bound States for Magic State Distillation in Fault-Tolerant Quantum Computation, *Phys. Rev. Lett.* **104**, 030503 (2010).
- [57] S. Cree, K. Dolev, V. Calvera, and D. J. Williamson, Fault-tolerant logical gates in holographic stabilizer codes are severely restricted, *PRX Quantum* **2**, 030337 (2021).
- [58] N. Rengaswamy, R. Calderbank, M. Newman, and H. D. Pfister, On optimality of CSS codes for transversal T , *IEEE J. Selected Areas Inf. Theory* **1**, 499 (2020).
- [59] E. Knill, R. Laflamme, and W. Zurek, Threshold accuracy for quantum computation, [arXiv:quant-ph/9610011](https://arxiv.org/abs/quant-ph/9610011).
- [60] J. T. Anderson, G. Duclos-Cianci, and D. Poulin, Fault-Tolerant Conversion between the Steane and Reed-Muller Quantum Codes, *Phys. Rev. Lett.* **113**, 080501 (2014).
- [61] C. Cao, J. Pollack, and Y. Wang, Hyper-invariant MERA: Approximate holographic error correction codes with power-law correlations, *Phys. Rev. D* **105**, 026018 (2022).
- [62] C. Cao and B. Lackey, Building quantum error correction codes from tensor networks, [arXiv:2109.08158](https://arxiv.org/abs/2109.08158).
- [63] B. Zeng, H. Chung, A. W. Cross, and I. L. Chuang, Local unitary versus local Clifford equivalence of stabilizer and graph states, *Phys. Rev. A* **75**, 032325 (2007).